

# Microstructural development during aging of 2014 aluminum alloy composite

S. K. VARMA, D. SALAS, E. CORRAL, E. ESQUIVEL

*Department of Metallurgical and Materials Engineering, The University of Texas at El Paso, El Paso, Texas 79968-0520, USA*

*E-mail: skvarma@mail.utep.edu*

K. K. CHAWLA

*Materials and Mechanical Engineering Department, The University of Alabama at Birmingham, Birmingham, AL 35294-4461, USA*

R. MAHAPATRA

*Naval Air Warfare Center, Aircraft Division, Patuxent River, Maryland 20670-1908, USA*

The 2014 aluminum alloy reinforced with 0.1 and 0.15 volume fraction of alumina particles (VFAP) have been solutionized for a range of time from 1.5 to 20 h at 813 K. The effect of solutionizing time (ST) on the age hardening response of the composites has been studied and compared with the characteristics exhibited by the monolith. The results indicate that increasing the ST decreases the time required to get the peak hardness (TPH) values in the monolith but the composites do not show a systematic monotonic behavior. The TPH values first decrease and then increase with an increase in ST at an aging temperature of 473 K for the composite. It has been speculated that the ST influences the concentration of quenched-in vacancies and continued heating may affect the bonding between particles and matrix which can generate additional dislocations throughout the solutionizing process due to curvature effects. © 1999 Kluwer Academic Publishers

## 1. Introduction

The effect of solutionizing time (ST) at 813 K on the aging behavior of 6061 aluminum alloy and its composites reinforced with 0.10, 0.15 and 0.20 volume fractions (VFAP) of alumina particles has been studied recently [1–4]. The time required to get the peak hardness (TPH) values was observed to be such that it decreases with an increase in ST in the monolith at 433, 453, 473 and 493 K. The TPH values, however, first decrease and then increase with an increase in ST at similar aging temperatures but it was confirmed that there is an accelerated aging in the composites under identical heat treatment conditions as reported in the literature by many authors [5–12].

The solutionizing of alloys result in the grain growth process which follows the parabolic dependence on time in both 2014 monolith and its composites containing 0.10 and 0.15 VFAP [3]. A graph between the square of the solutionized grain size as a function of time at the solutionizing temperature indicates almost similar slopes for 0.10 and 0.15 VFAP but the composite containing 0.20 VFAP shows two different slopes for the range of ST from 1.5 to 20 h. The decohesion of the particles in the initial stages of the solutionizing process has been confirmed in all the three composites but the coalescence of the particle could only be observed in 0.20 VFAP composite at longer times and indicated an increase in grain growth rate accompanying this stage of solutionizing. Another significant effect of

grain growth is to emit vacancies as a result of decrease in grain boundary surface area [2–4].

The TEM of the solutionized samples indicate an increase in dislocation density at both the particle matrix interface (will now be referred to as interface) and the areas away from the interface (will now be referred to as matrix) as a function of ST. The differences in the values of the coefficient of thermal expansion (CTE) between the matrix and particles alone can not account for the CTE dislocation generation during the entire range of solutionizing time, up to nearly 20 h. The improvement in bonding between the particles and the matrix as a result of continued heating for long periods of time during solutionizing can give rise to interface curvature effect and can be responsible for a monotonic increase in dislocation density [1].

The monolith of 2014 aluminum alloys show different types of phases that are formed during the aging process. It must be noted that the alloy undergoes the usual sequence of GP zones [13–15] besides the formation of few specific phases. A quaternary  $\text{Al}_5\text{Cu}_2\text{Mg}_8\text{Si}_5$  with a hexagonal crystal structure ( $a = 10.30 \text{ \AA}$  and  $c = 4.04 \text{ \AA}$ ) has been assigned the symbol  $\lambda$  and also has its counterpart as metastable phase  $\lambda'$  [13]. S-phase is yet another important phase with a stoichiometry of  $\text{Al}_2\text{CuMg}$  has an orthorhombic crystal structure. The presence of  $\theta$  phase with chemical formula of  $\text{CuAl}_2$  is quite well recognized in the literature and has a tetragonal crystal structure with its metastable forms  $\theta''$  and  $\theta'$ .

Dutta and his coworkers [13–15] have concluded that there are two important nucleation sites for precipitation to occur during aging of the composite materials: quenched-in vacancies and the CTE dislocations especially for 2014 alloys and composites containing alumina particles. The effect of ST on these two parameters, as discussed above, would then indicate that their concentrations may change and there may be an influence on the kinetics of the precipitation process during aging. It is the purpose of this research to present the results on 2014 aluminum alloy in the monolithic form and the composite containing 0.10 and 0.15 VFAP showing the effect of these two parameters affecting the aging curves at 433, 453, and 473 K.

## 2. Experimental details

The composites of 2014 aluminum alloy reinforced with 0.10 and 0.15 VFAP, with particle sizes of 10 and 15  $\mu\text{m}$  respectively, were purchased from Duralcan, Inc. in the form of an extruded rod of 12.5 mm diameter. The alloy in the monolithic form was obtained from a local source. The nominal composition of a typical commercial 2014 aluminum alloy consists of 4.0% Cu, 0.5% Mg, 0.8% Si, while 6061 aluminum alloy has 1.0% Mg, 0.6% Si, 0.2% Cr and 0.3% Cu and the balance being aluminum.

The heat treatment of the alloys and composites was carried out in air using a box furnace with a thermocouple attached to the specimen. The solutionizing was done at 813 K and the samples were quenched in room temperature water. The storing of the samples, when not in use, was always done in a freezer. The same furnace was also used for aging the solutionized samples for various lengths of time ranging from few minutes to 5000 min. The samples were quenched in room temperature water even after aging treatment.

Shimadzu microhardness testing machine was used for the measurement of hardness values. Six or seven readings were taken for each hardness value and the average has been used to plot the aging curves throughout this paper. It must be noted that the hardness readings were taken in such a way so as to include particles in the location of the indentation and a load of 500 g was used. This would correctly represent the overall hardness reading for the composite.

The TEM sample preparation technique involved cutting a sample of 0.5 mm from the rods of the composite and then hand grinding them down to 0.3 mm. A disc of 3 mm diameter was punched out from the wafer using a hand punch and hand ground to a thickness of 0.15 mm. A GATAN dimpler was used to dimple the 0.15 mm thick hand ground samples on both sides giving a final thickness of about 50  $\mu\text{m}$  in the middle. The ion milling of the sample was then carried out using a GATAN ion mill at 4 kV, current of 1 mA and a beam inclination of 12 deg to the specimen. Once the hole has been detected in the sample it was placed in a Hitachi H-8000 Scanning Transmission Electron Microscope (STEM) for microstructural examination using an accelerating voltage of 200 kV.

The TEM samples from the monolith were made by the standard dual jet electropolishing technique. A

Struer's Tenupol-3 electropolisher was used with a solution consisting of 30% nitric acid and 70% methanol at 253 K. The final rinse was done in water and then methanol was used for quick drying.

## 3. Results and discussion

### 3.1. Solutionizing

The effect of solutionizing at 813 K on the development of microstructures in 2014 aluminum containing 0.10 and 0.15 VFAP can be seen in Figs 1 and 2, respectively. It can be seen that the grain sizes are, in general, larger with lower VFAP and the distribution of particles becomes more uniform with increase in solutionizing time. The decrease in particle size as a function of solutionizing time due to decohesion process reported earlier by the authors of this group [1] for 6061 aluminum alloys containing various VFAP has not been observed in this material under almost identical conditions. However, coalescence of the particles in the composite with 0.15 VFAP is quite apparent from the optical micrographs shown in Fig. 2. A decrease in hardness values as a function of time of solutionizing has been observed in 2014 aluminum composites [2, 3]. It must be noted that relatively large grain sizes can be obtained by the solutionizing process which is contrary to the belief that grain size control in composites is rather unusual.

### 3.2. Aging

Fig. 3 shows aging curves at 433, 453 and 473 K for 2014 aluminum alloy in the monolith form as well as when reinforced with 0.10 VFAP. The higher hardness values for the composites, in general (except at 473 K for a solutionizing time of 20 h), is quite noticeable. There are two important features of the aging curves that must be noted from Fig. 3. First, the time required to get the peak hardness (TPH) values decrease with increase in aging temperatures which is to be expected since higher temperature promotes the aging process. The authors believe that the TPH at 433 K has not been achieved in this study even after aging for about 5000 min. Second, Table I shows that the TPH values for the monolith is such that it also decreases with increase in solutionizing time at a given aging temperature e.g., decreases from 380 to 50 min at 473 K, while the composite does not show such a consistent behavior. It must be noted that 6061 aluminum alloy composites show a decrease and then increase in TPH values with an increase in solutionizing time as shown in Fig. 4 [2–4] while the monolith behaves in a manner identical to the results of 2014 aluminum alloy of this study (see Table II). The comparison of aging curves for the composites

TABLE I TPH (in minutes) values for 2014 aluminum and 0.10 VFAP composite

|       | 2014 Aluminum alloy monolith |      |      | 0.10 VFAP composite |     |      |
|-------|------------------------------|------|------|---------------------|-----|------|
|       | 1.5 h                        | 5 h  | 20 h | 1.5 h               | 5 h | 20 h |
| 453 K | 2000                         | 2000 | 1500 | 250                 | 170 | 850  |
| 473 K | 380                          | 250  | 50   | 100                 | 100 | 170  |

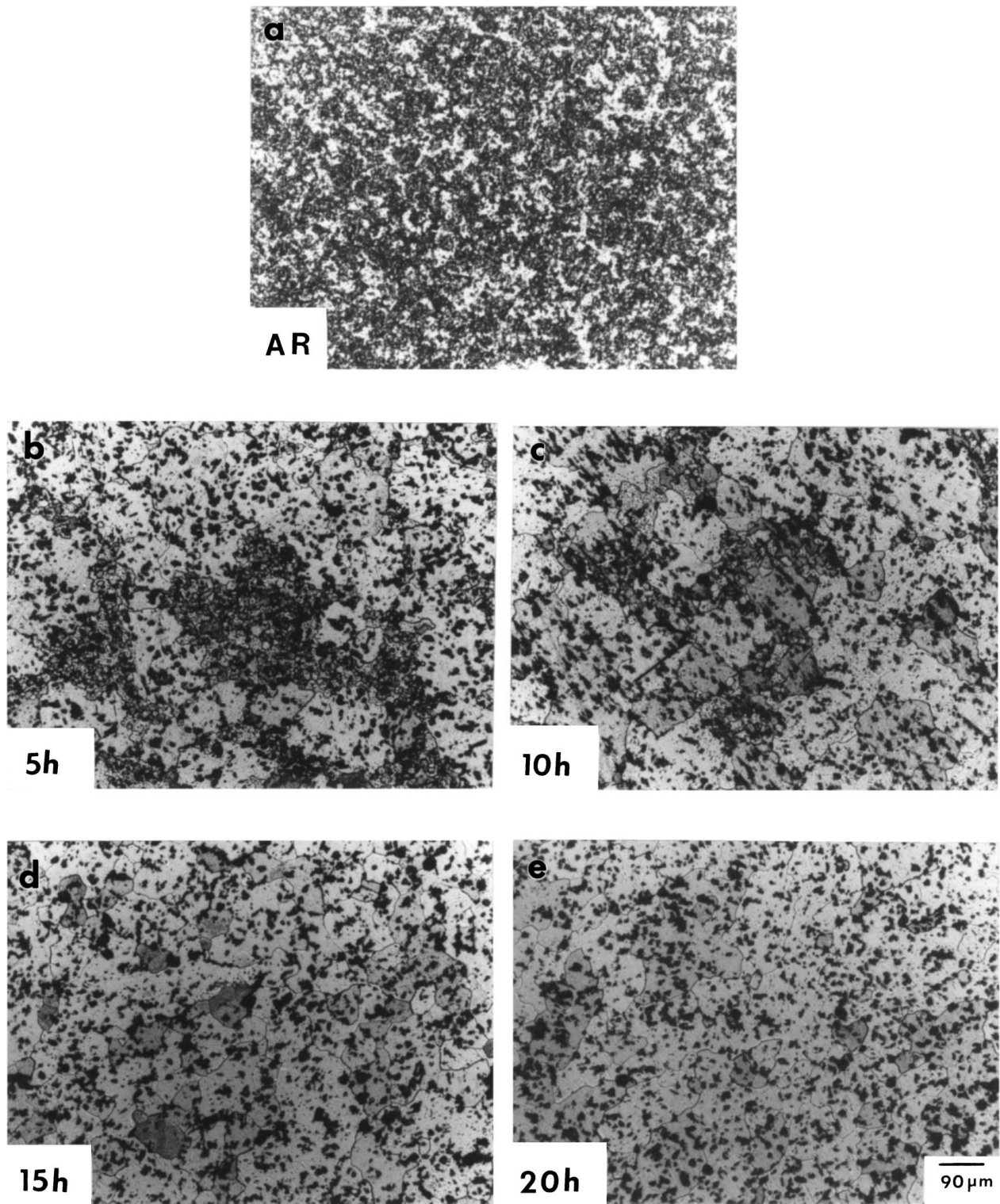


Figure 1 The microstructures observed, by optical microscopy, after solutionizing 2014 aluminum alloy composite reinforced with 0.10 VFAP at 813 K for (a) as received condition, (b) 5, (c) 10, (d) 15, and (e) 20 h.

TABLE II TPH (in minutes) values for 6061 aluminum and 0.10 VFAP composite

|       | 2014 Aluminum alloy monolith |      |      | 0.10 VFAP composite |     |      |
|-------|------------------------------|------|------|---------------------|-----|------|
|       | 1.5 h                        | 5 h  | 20 h | 1.5 h               | 5 h | 20 h |
| 453 K | 3500                         | 1500 | 500  | 3500                | 100 | 500  |
| 473 K | 380                          | 500  | 200  | 380                 | 100 | 1000 |
| 493 K | 250                          | 170  | 50   | 250                 | 50  | 250  |

containing 0.10 and 0.15 VFAP with the monolith at 473 K is shown in Fig. 5. The decrease in TPH value with increase in VFAP in the composites can be seen for samples solutionized only for 1.5 h as shown in Table III. In fact, it increases with particles size for samples solutionized for 5 and 20 h. The effect of particle size on the TPH values (at an aging temperature of 473 K) as observed by the authors of this paper and the data obtained from Dutta *et al.* [13] at 458 K can be seen in Table IV for solutionizing times of 1.5 and 1 h

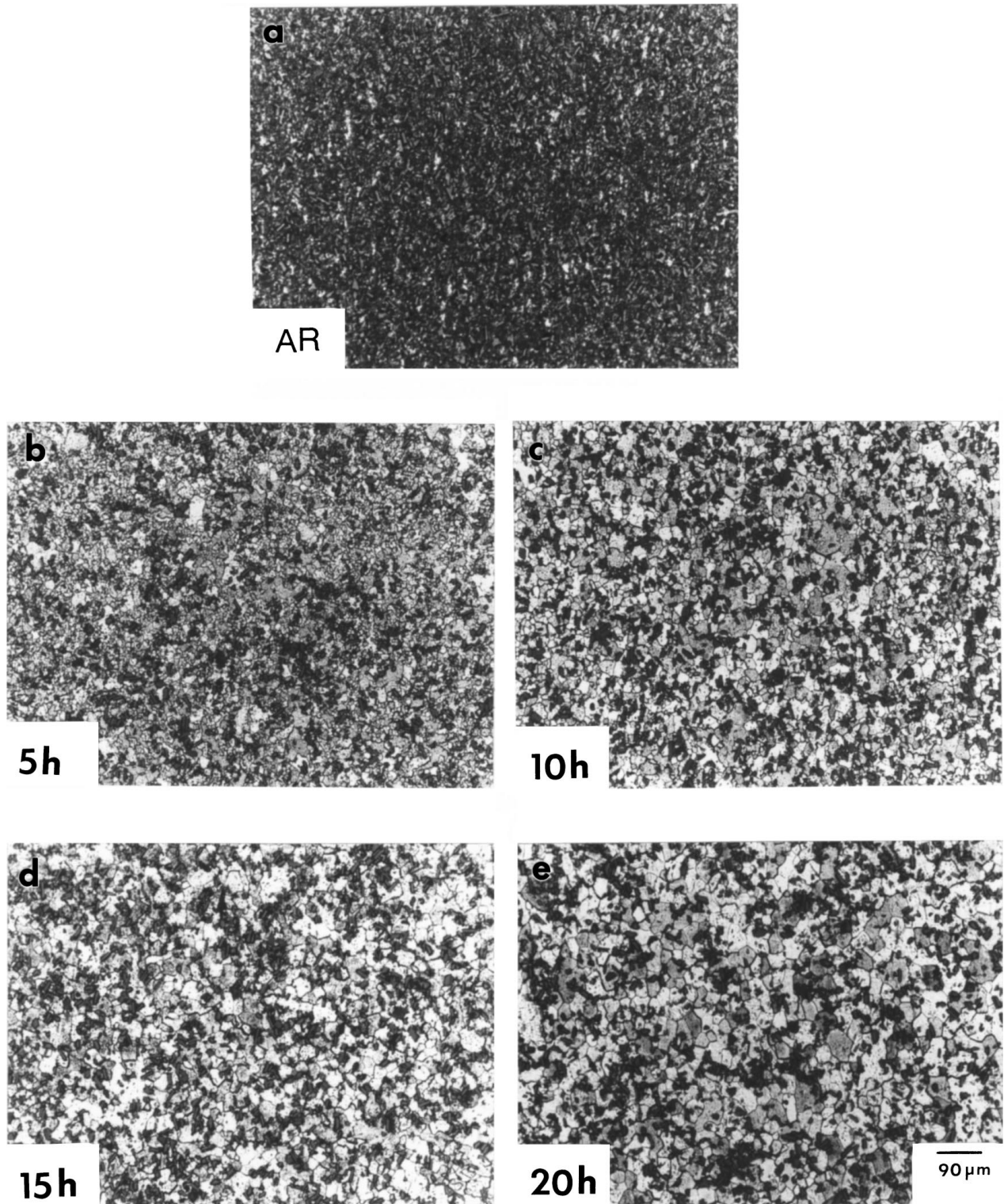


Figure 2 The microstructures observed, by optical microscopy, after solutionizing 2014 aluminum alloy composite reinforced with 0.15 VFAP at 813 K for (a) as received condition, (b) 5, (c) 10, (d) 15, and (e) 20 h.

TABLE III Comparison of TPH values (in minutes) for monolith and composites at 473 K

|               | 1.5 h | 5 h | 20 h |
|---------------|-------|-----|------|
| 2014 Aluminum | 380   | 250 | 50   |
| 0.10 VFAP     | 100   | 100 | 170  |
| 0.15 VFAP     | 100   | 850 | 850  |

TABLE IV TPH value comparison with published [13] results

| Material         | Aging temperature (200 °C) | Aging temperature (185 °C) <sup>a</sup> |
|------------------|----------------------------|---|
| 2014             | 500 min                    | 380 min                                 |
| 2014 + 0.10 VFAP | 150 min                    | 100 min                                 |
| 2014 + 0.15 VFAP | 100 min                    | 100 min                                 |

<sup>a</sup>Results from this research for a solutionizing time of 1.5 h.

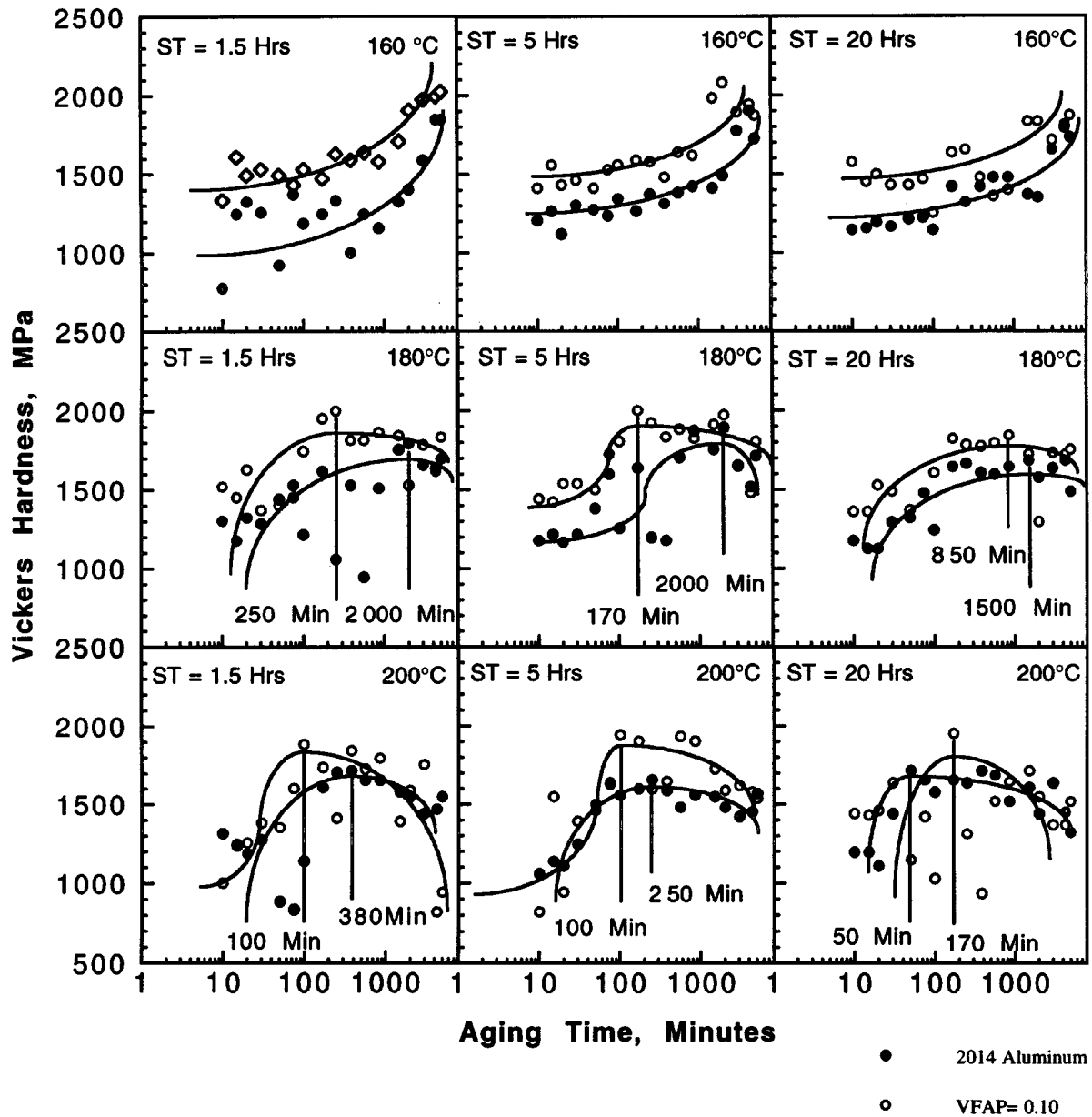


Figure 3 Aging curves of 2014 aluminum alloy in the monolith form and reinforced with 0.10 VFAP for solutionizing time of 1.5, 5 and 20 h (columns) at 433, 453 and 473 K (rows).

respectively. This table shows that the TPH value decreases or stabilizes with an increase in solutionizing time and the results appear to be quite reproducible.

### 3.3. Microstructures during aging at 473 K

The microstructural development taking place during aging treatment at 473 K for samples solutionized for 1.5 and 20 h has been shown in Fig. 6 in the peak hardened (PH) condition for the composite. The existence of needles of  $\lambda'$  and GP 2 zones in extremely small sizes are the main microstructural features in the PH condition for 1.5 h of solutionizing time while rather well developed  $\lambda'$  and  $\theta'$  for the 20 h of solutionizing treatment have been observed. The accelerated aging response of the composites with longer solutionizing time at a given temperature of solutionizing may be attributed to the increased number of nucleation sites for the precipitation to occur.  $\theta'$  has been shown to be nucleated at the dislocations and it has been observed that

higher amount of  $\theta'$  forms in the composites compared to the monolith due to the generation of CTE dislocations during solutionizing [13]. A similar increase in CTE dislocation density in the composites of 2014 aluminum alloy reinforced with alumina particles may also be assumed which can provide for the explanation of accelerated aging response of this study when solutionized for longer time. A decrease in hardness value with increase in solutionizing time may still be possible, even with the assumption of increase in CTE dislocation density, if the softening produced by the grain size coarsening is larger than the hardening produced by an increase in dislocation density.

The competing mechanisms for nucleation of precipitates in the solutionized samples can give rise to the inconsistent behavior of TPH variation with solutionizing time. It may be due to the fact that the kinetics of quenched-in vacancies and CTE dislocation generation may not be identical and, in fact, the formation of precipitates involves the competition between the CTE

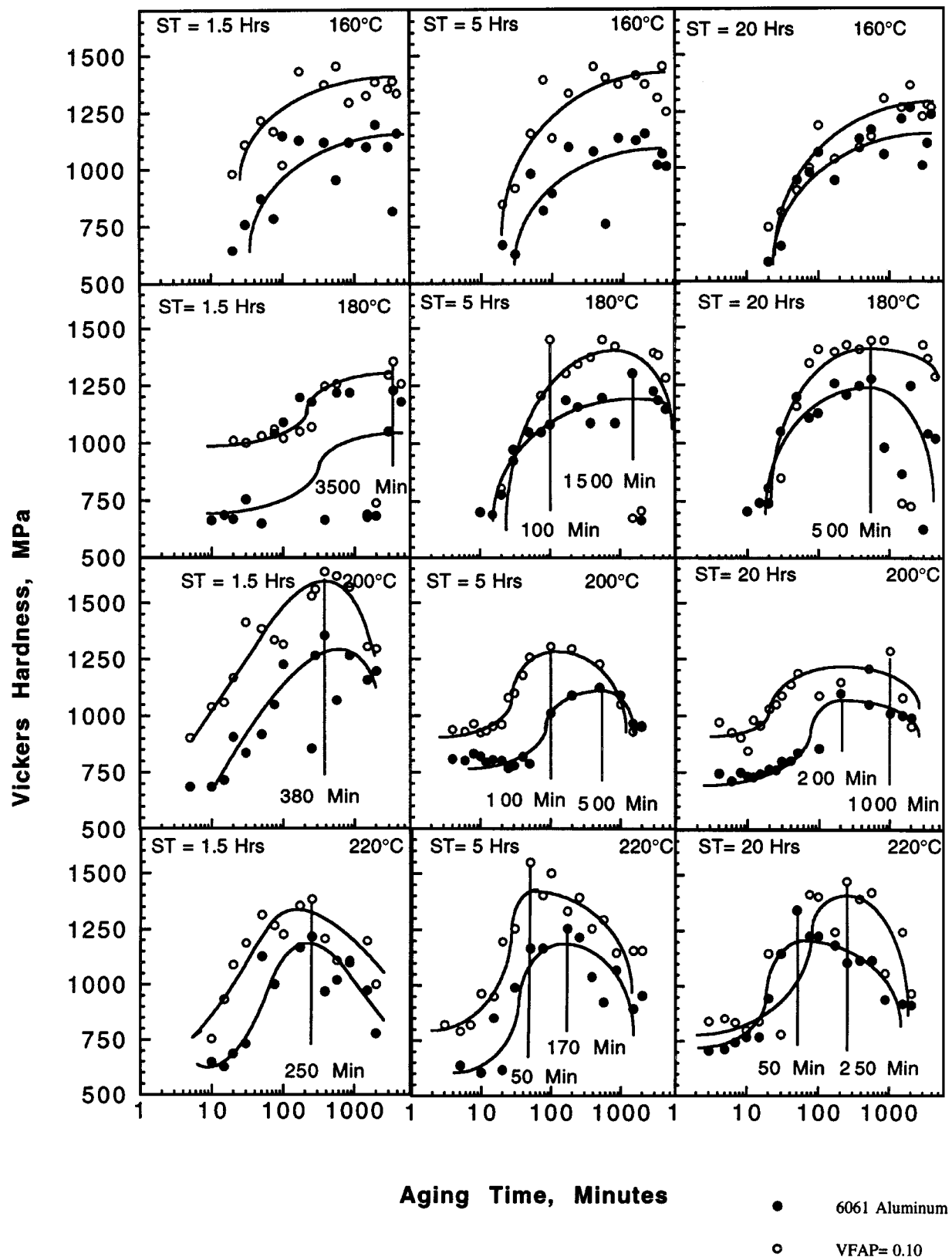


Figure 4 Aging curves of 6061 aluminum alloy in the monolith form and reinforced with 0.10 VFAP for solutionizing time of 1.5, 5 and 20 h (columns) at 433, 453, 473, and 493 K (rows) [2–4].

dislocations and vacancies as nucleation sites. It may be assumed that the CTE dislocation nucleation sites will be consumed first and then the vacancies may be absorbed to initiate the nucleation process. However, it must be noted that such a model does not prevent the formation of GP zone sequence which uses the vacancies cluster to attract the Si atoms to form silicon rich

clusters (SRC) and then Mg atoms may be transported either through lattice or pipe diffusion to such SRCs. It is possible that the dislocations as well as vacancies may be used as a nucleation site at the same time.

Fig. 7 shows the morphology and density of precipitates formed for the samples of 2014 aluminum alloy reinforced with 0.15 VFAP solutionized for 20 h in the

TABLE V DSC results on 2014 alloy and 0.15 VFAP composite for  $\theta'$  formation

| Materials | Solutionizing time (5 h) |                  | Solutionizing time (10 h) |                  | Solutionizing time (20 h) |                  |
|-----------|--------------------------|------------------|---------------------------|------------------|---------------------------|------------------|
|           | Temp (°C)                | $\Delta H$ (J/g) | Temp (°C)                 | $\Delta H$ (J/g) | Temp (°C)                 | $\Delta H$ (J/g) |
| 2014      | xx                       | xx               | 268.7                     | 16.56            | 264.8                     | 27.46            |
| 0.15 VFAP | 268.8                    | 6.84             | 265.8                     | 8.51             | 264.6                     | 9.31             |

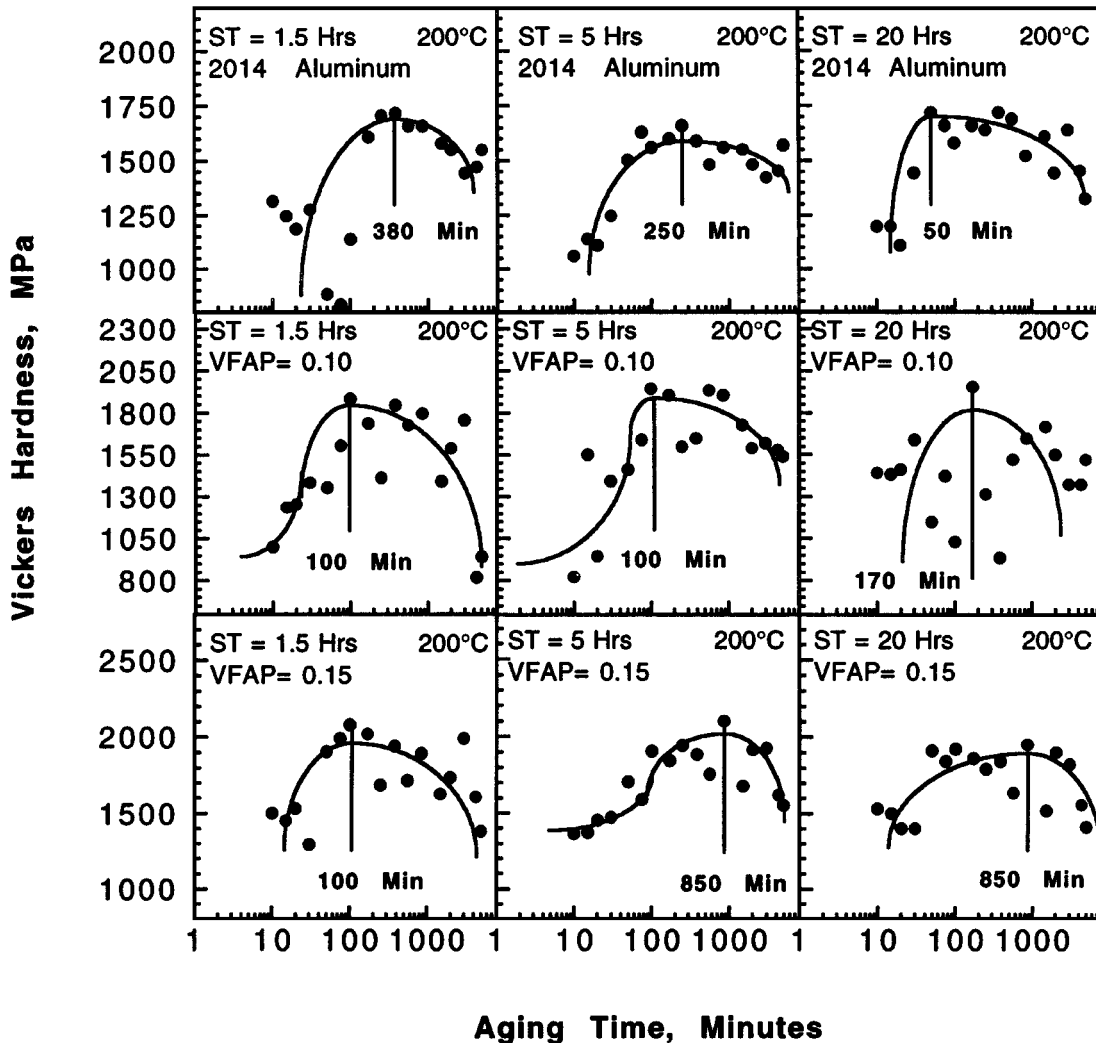


Figure 5 A comparison of the aging curves of the 2014 aluminum alloy in the monolithic form, and composites containing 0.10 and 0.15 VFAP at 473 K for solutionizing times of 1.5, 5 and 20 h.

PH and OA conditions. The coalescence of precipitates from the PH to OA state can be easily recognized. This may suggest that  $\theta'$  precipitates simply coalesce along their longer interfaces. The figure shows some of the precipitates that have sizes similar to those observed in the PH condition indicating that these precipitates have not yet taken part in the growth of the precipitates by coalescence. The short ends of the precipitates do not appear to contribute to the coarsening process during aging and the duplex orientation shown in Fig. 6b may be only due to the multiple orientations available for the habit planes.

### 3.4. DSC results

Thus the accelerating aging response with respect to the increase in solutionizing time shown in this study

can be considered to be due to the increase in concentration of vacancies and CTE dislocation density, both of which may act as the nucleation site for the precipitates to form during aging treatment. Table V shows the differential scanning calorimetry (DSC) (scanned at 10 K/min) results for 2014 aluminum alloy and a composite containing 0.15 VFAP for samples solutionized for 5, 10 and 20 h. The results are indicated for the  $\theta'$  formation only. It can be clearly seen that the temperature of formation decreases with an increase in solutionizing time for both monolith and composite even though the magnitude of decrease in the temperature is rather small. It must be noted that the data for 5 h of solutionizing of the monolith could not be obtained due to some instrumentation problems. The enthalpy ( $\Delta H$ ), refers to the heat of formation, values show a more dramatic effect. The  $\Delta H$  values increase from



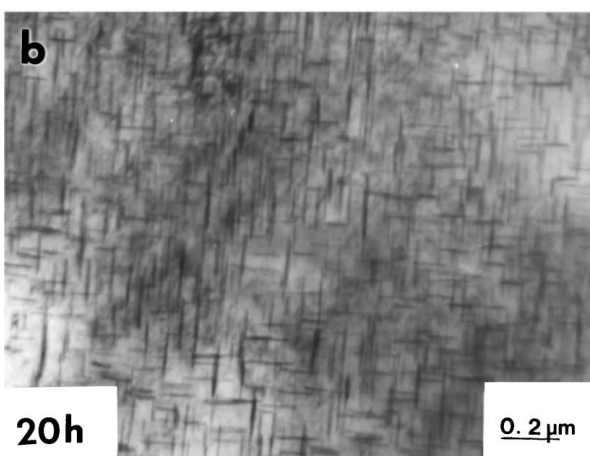
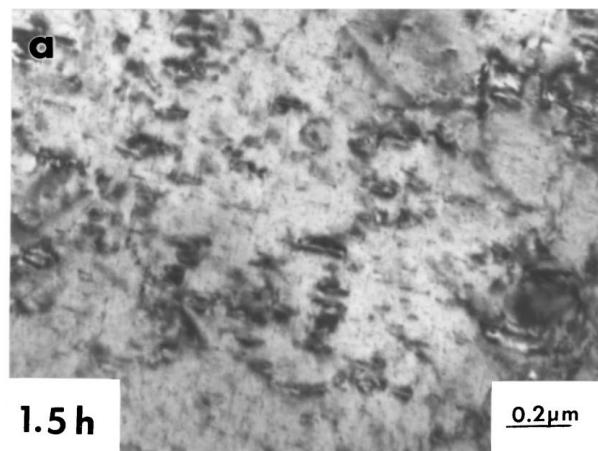


Figure 6 TEM of the microstructures evolved in 2014 aluminum alloy reinforced with 0.15 VFAP during aging at 473 K for a solutionizing time of (a) 1.5 and (b) 20 h in the peak hardened condition.

6.84 to 9.31 J/g as the solutionizing time changes from 5 to 20 h. The decrease in temperature for  $\theta'$  and an increase in  $\Delta H$  value as a function of solutionizing time both support our TEM observations and the concept of competing nucleation mechanisms for CTE dislocations and quenched-in vacancies in the form of TPH variation and accelerated aging response of composites.

#### 4. Conclusions

1. Grain growth process during solutionizing of 2014 aluminum alloy reinforced with alumina particles occurs in a manner similar to that observed for 6061 aluminum alloy also reinforced with alumina particles of similar sizes and volume fractions.

2. Increase in solutionizing time at 813 K for 2014 aluminum alloy in the monolithic form results in decrease in time required to get the peak hardness values during aging at 433 and 453 K.

3. The composite with 0.10 VFAP does not show a systematic variation in TPH value with solutionizing time during aging.

4. A competition between the quenched-in vacancies and generation of CTE dislocations for nucleation sites during aging may be responsible for the differences in the aging behavior between the monolith and composites.

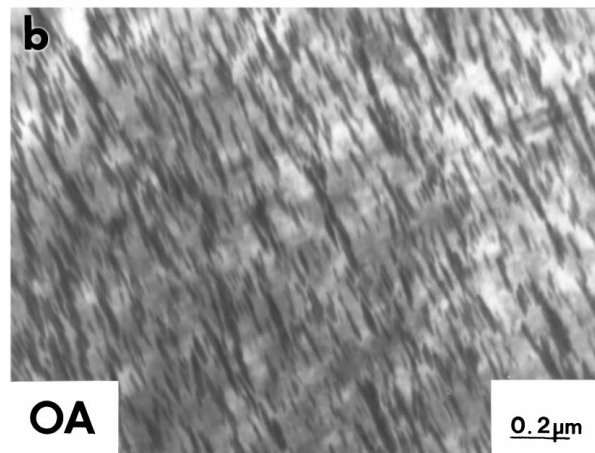
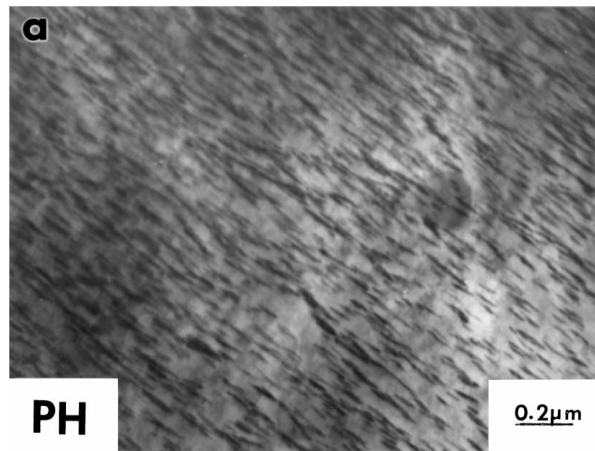


Figure 7 TEM of the microstructures evolved in 2014 aluminum alloy reinforced with 0.15 VFAP during aging at 473 K for a solutionizing time of 20 h in the (a) peak hardened and (b) overaged condition showing the coalescence of precipitates.

5. However, the aging response of composites may be attributed to the availability of the additional nucleation sites in comparison with those available for the monolith.

#### Acknowledgement

The authors wish to acknowledge the financial support of National Science Foundation through the grant number HRD-9353547.

#### References

1. S. K. VARMA, J. PONCE, M. SOLIS, S. ANDREWS and D. SALAS, *Metallurgical and Materials Transactions A* **27A** (1996) 2023–2034.
2. S. K. VARMA, J. PONCE, E. CORRAL and D. SALAS, in "Processing, Properties and Applications of Cast Metal Matrix Composites," edited by P. K. Rohatgi (TMS-AIME, Warrendale, PA, 1996) pp. 67–76.
3. S. K. VARMA, D. SALAS, J. PONCE, E. CORRAL, E. ESQUIVEL and M. REGALADO, in "Light Weight Alloys for Aerospace Applications," edited by E. W. Lee, K. Jata, W. E. Frazier and N. J. Kim, P. K. Rohatgi (TMS-AIME, Warrendale, PA, 1997) pp. 287–296.
4. S. K. VARMA, in "Thermomechanical Processing of Steel and Other Materials," THERMEC'97, edited by T. Chandra (TMS-AIME, Warrendale, PA, 1997) pp. 1359–1365.
5. K. K. CHAWLA, A. H. ESMAELI, A. K. DATYE and A. K. VASUDEVAN, *Scripta Metallurgica*, **25** (1991) 1315–1319.



6. R. J. ARSENAULT and R. M. FISHER, *ibid.* **17** (1983) 67–71.
7. I. DUTTA, D. L. BOURELL and D. LATMER, *J. Compos. Materials* **22** (1988) 829–849.
8. T. CHRISTMAN, A. NEEDLEMAN and S. SURESH, *Mater. Sci. Eng.* **A107** (1989) 49.
9. T. CHRISTMAN, A. NEEDLEMAN and S. SURESH, *Acta Metall.* **37** (1989) 3029–3050.
10. T. CHRISTMAN and S. SURESH, *ibid.* **36** (1988) 1691–1704.
11. J. M. PAPA ZIAN, *Metall. Trans. A* **19A** (1988) 2945–2953.
12. T. G. NIEH and R. F. KARLAK, *Scripta Metallurgica* **18** (1984) 25–28.
13. I. DUTTA, C. P. HARPER and G. DUTTA, *Metall. and Mater. Trans. A* **25A** (1994) 1591–1602.
14. I. DUTTA, S. N. ALLEN and J. L. HAFLEY, *Metall. Trans. A* **22A** (1991) 2553–2563.
15. I. DUTTA and D. L. BOURELL, *Acta Metallurgica et Materialia* **38** (1990) 2041–2049.

*Received 12 October 1997  
and accepted 26 October 1998*